Delayed response of human melanopsin retinal ganglion cells on the pupillary light reflex

Sei-ichi Tsujimura and Yuta Tokuda

Department of Information Science and Biomedical Engineering, Kagoshima University, Kagoshima, JAPAN

ABSTRACT

A recent study has shown that retinal ganglion cells containing the photopigment melanopsin, which are intrinsically photosensitive in primates, project to the pupillary control center in the pretectum. The aim of this study was to investigate how melanopsin retinal ganglion cells (mRGCs) contribute to the pupillary pathway. We designed and built a novel multi-primary stimulation system to control stimulation of the three cone types and mRGCs independently in the human eye. We measured a latency and amplitude of transient pupillary responses to three types of test stimuli modulating excitations of mRGCs and cones (mRGC, luminance and the light flux stimuli). It was found that the transient pupillary response to mRGC stimuli has a longer latency than that to luminance and the light flux stimuli when an onset of sinusoidal stimulus was used. The results indicate that we successfully demonstrated the pupillary response to mRGCs under conditions where mRGCs are isolated in humans. Furthermore, the data confirm that the delayed response disappeared when the stimulus is presented as a square-wave pulse and not weighted by a sinusoid. The similarity of time courses for the earlier phase of pupillary responses to all stimuli suggested that these transient pupillary responses were driven by a single mechanism, which is perhaps associated with cone-mediated signals.

Keywords: human, pupil, melanopsin, cone, silent-substitution

Running head: Delayed pupillary response of human melanopsin ganglion cells

Correspondence to Sei-ichi Tsujimura

Tel&Fax: +81-(0)99-285-8488

Email address:tsujimura@ibe.kagoshima-u.ac.jp

INTRODUCTION

In the conventional view of retinal physiology, rods and cones are assumed to be the only photoreceptors in the eye. Therefore, in addition to their photoreceptive function, they were considered responsible for non-image forming processing such as pupillary light reflex and photoentrainment. To clarify whether classical photoreceptors are responsible for non-image forming processing, researchers have generated transgenic mice that lack all functional rod and cone photoreceptors. These mice showed normal suppression of pineal melatonin (Lucas et al, 1999) and phase-shifting response to light (Freedman et al, 1999), indicating that another type of photoreceptor that plays a role in non-image forming processing must be present within the eye. Furthermore, these mice exhibited pupillary constriction in response to intense light (Lucas et al, 2001), suggesting that the novel photoreceptor does more than merely regulate the circadian system.

The novel opsin, melanopsin, was identified by Provencio and colleagues (Provencio et al, 1998; Provencio et al, 2000). Berson et al. showed that intrinsically photosensitive retinal ganglion cells containing the photopigment melanopsin transmit information to the suprachiasmatic nucleus (SCN) of the hypothalamus (Berson et al, 2002). Several researchers have described the anatomical and physiological features of the novel melanopsin-containing retinal ganglion cells (mRGCs); they are sparsely distributed in

the retina (Provencio et al, 2002), have an action spectrum peaking at ~480 nm (Lucas et al, 2001; Berson et al, 2002; Dacey et al, 2005; Gamlin et al, 2007) or ~460 nm (Brainard et al, 2001; Thapan et al, 2001), and a single absorbed photon is sufficient for generating spikes as rods (Do et al, 2009). The mRGCs have a sustained response with a long latency to intense stimuli (Berson et al, 2002; Dacey et al, 2005) and much slower than cones (Lucas et al, 2001; Berson et al, 2002; Lall et al, 2010). These cells also have giant dendritic fields that receive cone-mediated onset and offset signals which are organized as a color-opponent receptive field (Dacey et al, 2005) and convey brightness information to the SCN and other non-image forming processing centers in the brain such as the olivary pretectal nucleus and the intergeniculate leaflet of the thalamus (Berson et al, 2002; Hattar et al, 2002). These particular brain centers receive irradiance information not only from the mRGC, but also from classical photoreceptors, rods and cones (Ruby et al, 2002; Panda et al, 2002; Lucas et al, 2003; Mrosovsky and Hattar, 2003; Hattar et al, 2003; Panda et al, 2003). Interestingly, melanopsin-knockout mice still show a pupillary response at low irradiance (Lucas et al, 2003) and maintain circadian rhythms (Ruby et al, 2002; Panda et al, 2002). On the other hand, melanopsin-knockout mice with degeneration of rods and cones (Panda et al, 2003), or with blockade of rod and cone functions (Hattar et al, 2003), exhibit a complete loss of

photoentrainment and the pupillary light reflex. These results clearly indicate that signals from both the mRGCs and the classical photoreceptors contribute to non-image forming functions.

In humans, it is difficult to investigate how signals from the classical photoreceptors and those from mRGCs are summed and contribute to non-image forming pathways. The challenge stems primarily from the need for selective stimulation of each photoreceptor type. For example, when pupil constriction was measured as a function of the level of light source emission, constriction occurred as the emission level increased, indicating that irradiance information was conveyed to the midbrain. In this case, pupil constriction can be explained by consolidated increases in excitation of the classical photoreceptors and mRGCs. One could use a monochromatic light of ~500 nm to selectively stimulate mRGCs. However, even when monochromatic light is used, classical photoreceptors are strongly stimulated, which induces luminance and color perception.

To isolate mRGC function, one could use subjects lacking functional rods and cones. For example, isolation of mRGC function was achieved in blind human subjects (Zaidi et al, 2007), in patients with retinitis pigmentosa (Kardon et al, 2010) and in transgenic animals lacking rods and cones (e.g., Lucas et al, 2001; Panda et al, 2002; Ruby et al,

2002; Lucas et al, 2003), and also by pharmacological blockade of rods and cones (Gamlin et al, 2007). Although these studies have shown that mRGCs contribute to pupil response, it is difficult to measure the contribution of mRGCs relative to cones using subjects with only mRGCs. Alternatively, it has been reported that one could measure a sustained pupil response (Gamlin et al, 2007; Young and Kimura, 2008; Kardon et al, 2009) or use long-duration test stimuli (McDougal and Gamlin, 2010) to achieve isolation of mRGC function, suggesting that the sensitivity of mRGCs is higher than that of cones at low temporal frequencies. McDougal et al. showed that mRGCs and rods contribute significantly to pupil constriction for test stimuli with duration of 100 s, whereas cones contribute only slightly, indicating that long-duration stimuli could be used to eliminate contamination by cones, but not rods. In a previous study, we measured steady-state pupil diameter in response to test stimuli modulating mRGC alone (Tsujimura et al, 2010). We used a silent-receptor substitution technique with a four-primary stimulation system to stimulate the mRGCs independently from the other photoreceptors. Pokorny and his colleagues showed the use of a four-primary system to investigate the rod-cones interactions (Shapiro et al, 1996; Pokorny et al, 2004; Cao et al, 2008). Here, we showed a significant change in steady-state pupil diameter when varying the excitation of mRGC alone, with no changes in luminance and color.

Furthermore, the change in pupil diameter by mRGCs was larger than that when luminance alone was varied, indicating that the mRGC signals contribute more than L- and M-cone signals to the pupillary pathway with a steady background.

In this study, we measured transient pupillary responses to test stimuli modulating the excitation of mRGCs and cones using a silent-substitution technique. For example, the test stimuli modulating the mRGCs varied only the mRGC excitation, while maintaining constant excitations of the three types of cones. The test stimuli induced no change in excitation in the three types of cones (i.e., “silent substitution”). In principle, it is straightforward to use 5 primaries to independently control the 5 types of receptors, that consists of 3 types of cones, rods and mRGCs, in the silent-substitution technique. However, since the peak of spectral sensitivity curve for mRGCs is close to that for rod it is essentially difficult to isolate mRGC only with silent-substitution technique (Vienot et al, 2010). We chose the intense background filed to avoid the rod contamination.

Silent substitution was used to isolate the target receptors. In addition, we used the onset of the sinusoidal stimuli to minimize the involvement of cones. We assumed that mRGCs are more responsive to the onset of sinusoidal stimuli whereas cones are more responsive to the onset of square-wave stimuli. We used the difference in temporal characteristics between the mRGCs and the cones as well as the silent-substitution

technique to isolate mRGC function.

The aim of this study was to investigate how signals driven by melanopsin-containing retinal ganglion cells and cone-mediated signals contribute to the pupillary control mechanism. We measured a latency and amplitude of transient pupillary responses to three types of test stimuli modulating excitations of mRGCs and cones. We showed that the pupillary response to mRGC stimuli with a smooth temporal envelope (i.e. sinusoidal stimuli) has a longer latency than the pupillary response to luminance and the light flux stimuli. On the other hand, no change in latency of pupillary response (given a similar time course) was found for any test stimuli with an abrupt temporal change (i.e. square-wave stimuli). These results showed that we successfully demonstrated the pupillary response to mRGCs under conditions where mRGCs are isolated in humans.

METHODS

Apparatus

A personal computer controlled a stimulation system (Fig. 1) consisting of two integrating spheres; one for test stimulus presentation and the other for background presentation. The test field comprised an annular ring and the background field comprised a circular field with a 23° diameter. We chose the annular ring for the test field to selectively stimulate mRGCs. The test field did not cover the fovea to avoid a

peak of cone distribution, but covered the peripheral field to include a peak of mRGC distribution.

The test stimulus was superposed on the background using a beam splitter. Four different kinds of light-emitting diodes (LEDs) were used as internal light sources in each integrating sphere. The peak wavelengths of the four LEDs were 633 nm, 599 nm, 524 nm, and 468 nm for test stimulus presentation and 596 nm, 517 nm, 500 nm, and 466 nm for background presentation. Half-height bandwidths for all LEDs ranged from 15 to 38 nm. The LEDs were manufactured by OptoSupplyLimited (Hong Kong, China). Luminance output of each LED was controlled by pulse width modulation (PWM) units by adjusting the duty cycle of the pulse train to 1 kHz. The PWM units were controlled by an embedded computer (H8/3052; Renesas Technology, Tokyo, Japan). The characteristics of duty-luminance and duty-amplitude were carefully calibrated to minimize the deviation caused by thermal effects (Watanabe et al, 1992). The spectral output of each LED was measured by a spectroradiometer (CS-1000A, KonicaMinolta, Tokyo, Japan). The head of the observer was held stable by a chin rest.

Figure 1

Stimuli

In all experiments, test stimuli were represented in a receptor-excitation space that used the excitations of three types of cones and mRGCs. The receptor-excitation space is a natural extension of the cone-excitation space, which uses three fundamentals corresponding to the excitation of each of the three kinds of retinal cones (Smith and Pokorny, 1996; Tsujimura et al, 2003; Tsujimura et al, 2007). The fundamentals were designed so that the total amount of excitation of long-wavelength sensitive cones (L cones) and middle-wavelength sensitive cones (M cones) was equivalent to the photopic luminous efficiency function V(λ). We used a fundamental for short-wavelength sensitive cones (S cones) with a unity peak of 1.0 to calculate S cone excitation. In addition to these three cone fundamentals, we used a spectral sensitivity curve for mRGC. These fundamentals were mapped onto four orthogonal axes in the receptor-contrast space. An excitation of mRGC was calculated from an estimated spectral sensitivity curve with a unity peak of 1.0. We assumed that neither the S cones nor the mRGC affect the photopic luminance efficiency function (i.e., luminance), despite using photopic luminance units (cd/m^2). The 10-deg cone fundamentals proposed by Stockman et al. (Stockman et al, 1999; Stockman and Sharpe, 2000) were used to calculate the excitation of each cone type. The ratio of energy peaks for L- and

M-cone was 1.98. We estimated the spectral sensitivity of mRGC from a pigment template nomogram (Dartnall, 1953) with a peak wavelength, λ_{max}, of 480 nm. Lucas et al. showed that a spectral tuning curve of mRGC as a function of wavelength was closely approximated by a pigment template with a peak at 480 nm (Lucas et al, 2001). The lens and macular pigment density spectra were those of Stockman et al. (Stockman et al, 1999). The fraction of incident light absorbed by the receptor depends on peak axial optical density (D_{peak}). Stockman et al. chose 0.38 for M and L cones and 0.30 for S cones. Despite a lack of relevant information, we tentatively chose 0.4 as the D_{peak} for mRGC as it was the same value as that for rods (Lamb, 1995). The resultant spectral sensitivity function of mRGC in a 10-deg field displayed a peak wavelength of 489 nm.

The CIE coordinate (CIE 1964) was (0.313, 0.535) for the background field and (0.460, 0.450) for the test field and the luminance values were 612 cd/m^2 and 1109 cd/m^2, respectively. The receptor excitation calculated from the fundamentals proposed by Stockman et al. for the test field was 816 cd/m^2 for L cones and 306 cd/m^2 for M cones. The receptor excitation for S cones and mRGC was 98 cd/m^2 and 692 cd/m^2, corresponding to 0.143 W/sr/m^2 and 1.013 W/sr/m^2, respectively. The retinal illuminance for the background field was 3.6 log photopic troland and 4.1 scotopic troland with a pupil size of 3.0 mm, which minimized the involvement of rods (Aguilar

and Stiles, 1954; Fuortes et al, 1961; Wyszecki and Stiles, 1982; Lee et al, 1997). Since the peak of spectral sensitivity curve for mRGCs is close to that for rod it is essentially difficult to isolate mRGC only with silent-substitution technique (Vienot et al, 2010). We chose the intense background filed to avoid the rod contamination, on the other hand, we chose the test field in order to provide a large receptor contrast for mRGCs in the silent-substitution paradigm. The retinal irradiance in photon flux was 13.8 log photons/cm^2/sec for the test field and 13.5 log photons/cm^2/sec for the background field. Notably, mice lacking rods and cones exhibited pupil constriction at this irradiance level (Lucas et al, 2001; Lucas et al, 2003). Since we used the intense background field it presumably produces large mRGC-mediated responses and less cone-mediated melanopsin responses due to saturation of cones (Lall et al, 2010).

We used three test stimuli as follows: varied mRGC excitation of the test stimuli alone (mRGC stimuli), varied luminance of the test stimuli alone (luminance stimuli), and varied radiant flux with no change in the spectral composition of the test stimulus, which reduced the radiant flux uniformly at all wavelengths (light flux stimuli). The mRGC stimulus had 0.08 Weber contrast for mRGCs while the contrast for the other receptors was null. The luminance contrast was 0.12 for the luminance stimulus. The luminance contrast was 0.12 and the mRGC contrast was 0.04 for the light flux stimulus.

The mRGC contrast of 0.08 was the maximum within the limitation of our apparatus. The other contrasts were chosen from the results of a preliminary experiment such that the response amplitude to each stimulus was approximately the same for all conditions to ensure an accurate comparison of latency of the response to the stimuli.

Procedure

Six visually corrected (with ultra-thin hydrophilic contact lenses) observers (age range 20–24 years) participated in the experiment. All observers had normal ocular health and normal color vision according to the Ishihara color blindness test. All observers gave their written informed consent, and the study was approved by the local research ethics committee. The observers were seated 25 cm from the diffuser and monocularly fixated upon a black Maltese cross, which subtended 1.8° and was always present at the center of the diffuser. The cross functioned as an accommodative 'lock,' providing a strong closed-loop stimulus to maintain accommodation at a constant level. After an initial adaptation period of 5 min, we began a session of experimental trials. The test stimulus was presented for 2 s. We used both onset of sinusoidal and square-wave, temporal envelopes to control the frequency content of the stimulus (Figure 2).

Figure 2

Figure 2 represents the temporal waveforms (upper panel) and the spectra (lower panel) for sinusoidal and square-wave stimuli. We used the onset of the sinusoidal stimuli to minimize the involvement of cones as they are more responsive to the high temporal frequency component (e.g., De Lange, 1954) that is characteristic of the abrupt change of the square-wave stimuli, but not of the sinusoidal stimuli.

The order of the test stimulus presentation was counter-balanced; one session lasted for approximately 40 min including an initial adaptation of 5 min, during which time observers were instructed to keep their right eye open, especially when the pupil diameter was recorded for periods of about 9 s. The left eye was masked throughout. Data were averaged from 60 traces in 2 sessions. The Student t-test with Bonferroni correction for multiple comparisons was used to compare pupillary responses to the three stimuli. All statistical analyses were done using a statistical analysis computer program (R Development Core Team, 2009).

Measurement of pupil size

The pupil of the right eye was imaged using a video camera (Dragonfly, Point Grey Research, Canada) located 0.5 m from the observer and 28° temporal to the visual axis.

The video image was fed into a personal computer and analyzed using LabVIEW and IMAQ Vision software (National Instruments) at a frequency of 60 Hz. The pupil was located using thresholding and edge detection techniques, allowing the pupil diameter to be analyzed at a resolution of <0.001 mm (Tsujimura et al, 2010).

Rod intrusion

It is possible that the transient pupillary responses could be caused by rods instead of mRGCs. Several researchers have shown that rod photoreceptor stimulation can produce large pupillary responses (e.g., Alpern and Ohba, 1972; Hansen and Fulton, 1986; McDougal and Gamlin, 2010). For example, McDougal et al. recently showed that both mRGCs and rods contribute significantly to pupil constriction for test stimuli with duration of 100 s, whereas cones contribute only slightly, suggesting rods could influence pupillary response. This is not the case in our experiments. McDougal et al. measured pupillary responses to a monochromatic light stimulus on the dark background field. Conversely, we measured pupillary responses to test stimuli superposed on the bright background field which minimized the involvement of the rods. The retinal illuminance of the background field was 3.6 log photopic troland and 4.1 scotopic troland, which effectively minimized the involvement of rods (Aguilar and Stiles, 1954; Fuortes et al, 1961; Wyszecki and Stiles, 1982; Lee et al, 1997). Aguilar

and Stiles showed that rod contamination is likely to diminish progressively above 100 scotopic trolands and be entirely absent at 2000–5000 scotopic troland in color-matching tasks (Aguilar and Stiles, 1954). This suggests that the rod contamination in our experiment was small or negligible.

RESULTS

Pupil responses to the onset of sinusoidal stimuli

Pupil responses to the onset of sinusoidal stimuli for two observers are shown in Fig. 3. The solid curve represents responses to the mRGC stimulus, the dotted curve represents responses to the luminance stimulus, and the broken curve represents responses to the light flux stimulus. The temporal envelope of the test stimuli is shown by the grey area on the time-scale axis. All test stimuli produced relatively large pupillary responses. The average pupil response was 0.19 ± 0.04 mm for the mRGC stimulus, 0.24 ± 0.03 mm for the luminance stimulus, and 0.21 ± 0.03 mm for the light flux stimulus. The latencies and amplitudes of the pupil response for all observers are summarized in Table 1. As we observed in the preliminary experiment, the response amplitudes of all three different stimuli were similar and no significant difference in response amplitude was found (all, $P>0.05$, paired t-test with Bonferroni's correction).

Figure 3

Results suggest that in all observers, the response to mRGC stimuli has a longer latency than the response to the luminance and light flux stimuli. The difference in latency in each response could be attributed to the difference in mechanism that induces the pupillary response. To investigate whether a different mechanism is involved in pupillary responses, the latency of the pupillary responses was analyzed and calculated using a normalization technique developed by Barbur et al. (Barbur et al, 1998). The amplitude of the pupillary responses to mRGC, luminance, and light flux stimuli were normalized with respect to the average amplitude and the trace was overlaid such that the difference in latency could be detected.

Figure 4 shows onset latencies and Fig. 5 shows the enlarged onset latencies for two observers. Times for the onset of pupil constriction for the mRGC stimuli ranged from 790 to 942 ms from the onset of the test stimulus with an average of 874±26 ms for all observers. The time for the onset of pupil constriction ranged from 614 to 774 ms for the luminance stimuli with an average of 697±25 ms, and from 626 to 757 ms for the light flux stimuli with an average of 685±21 ms. When the time for the onset of pupil constriction was compared among test stimuli, we consistently found that the latencies

for the mRGC stimuli were significantly longer than those for the luminance and light flux stimuli for all observers (P=0.0003 and 0.0002, paired t-test with Bonferroni's correction). Times for the onset of pupil constriction for the light flux and the luminance stimuli, on the other hand, were similar for all observers and no significant difference was found (P>0.05, paired t-test with Bonferroni's correction). The difference in latency could be due to a difference in the mediating mechanism, indicating that the latency of pupil response to the mRGC stimuli with onset of sinusoidal envelope was determined by mRGC signals, whereas the latency of pupil response to the luminance stimuli were determined by cone-mediated signals. The small difference in latency between luminance and the light flux stimuli suggested that these pupillary responses were determined by cone-mediated signals.

Figure 4

Figure 5

Similarly, times to peak constriction were analyzed to investigate whether a different mechanism mediates pupil response. Times to peak constriction from the onset of the

stimulus ranged from 1314 to 1772 ms for mRGC stimulus, 1114 to 1690 ms for the luminance stimulus, and 1114 to 1607 ms for the light flux stimulus. The average was 1557±63 ms for the mRGC stimuli, 1410±84 ms for the luminance stimuli, and 1426±71 ms for the light flux stimuli. The standard error of means for the time to peak constriction was approximately twice greater than that for the time for the onset of pupil constriction. When the time to peak constriction was compared among test stimuli, we found that there was no significant difference among these stimuli for all observers (all, $P>0.05$, paired t-test with Bonferroni's correction).

Time for the onset of pupil constriction for the mRGC stimuli was significantly longer than that for the luminance and light flux stimuli. The time course for the earlier phase of the response, therefore, may indicate mechanisms in which pupillary response are induced. The pupillary response to the mRGC stimuli could be driven by the mRGCs, whereas the similar time course of the luminance and light flux stimuli indicated that the responses to these stimuli were driven by cones, or possibly by cone-mediated post-receptoral mechanisms such as |L+M| luminance mechanism and |L-M| and |L+M-S| chromatic mechanisms. These signals could be associated physiologically with Magno-, Parvo- and Konio-cellular pathways. We shall return to this point in the Discussion.

Pupil responses to the square-wave stimuli

The pupil responses to the onset of square-wave stimuli for two observers are shown in Fig. 6. The temporal envelope of the test stimuli is shown by the grey area on the time-scale axis. All other details are the same as those in Fig. 3. All test stimuli produced relatively large responses. The average pupil response was 0.29 ± 0.03 mm for the mRGC stimulus, 0.34 ± 0.04 mm for the luminance stimulus, and 0.33 ± 0.04 mm for the light flux stimulus.

Figure 6

Figures 7 and 8 show onset latencies for two observers. The times for the onset of pupil constriction for mRGC stimulus ranged from 436 to 551 ms and the average was 483 ±17 ms for all observers. The time for the onset of pupil constriction ranged from 436 to 534 ms for the luminance stimulus with an average of 475±14 ms, and from 420 to 534 ms for the light flux stimulus with an average of 475±15 ms. When the time for the onset of pupil constriction was compared among the three test stimuli, we found that there was no significant difference among these stimuli (all, $P>0.05$, paired t-test with

Bonferroni's correction). The similarity in latency suggested that the pupillary responses to all stimuli were determined mostly by a single mechanism.

Similarly, times to peak constriction were analyzed to investigate whether a different mechanism mediates pupil responses. The times to peak constriction ranged from 838 to 1100 ms for mRGC stimulus, 852 to 1067 ms for the luminance stimulus, and 852 to 1067 ms for the light flux stimulus. The average was 949±36 ms for the mRGC stimulus, 958±28 ms for the luminance stimulus, and 949±28 ms for the light flux stimulus. When the time to peak constriction was compared among test stimuli, we found that there was no significant difference among stimuli (all, $P>0.05$, paired t-test with Bonferroni's correction).

There was no significant difference in either time for the onset of pupil constriction or time to peak constriction for all stimuli. Moreover, as shown in Figs. 6–8 the time courses for all stimuli were quite similar. These results indicate that a single mechanism drove the pupillary responses for all stimuli. One of the possible mechanisms could be a mechanism that mediates cone signals. Since sensitivity of cones is higher than that of mRGC at a high temporal frequency, pupillary responses to the square-wave stimuli were probably determined by cone-mediated signals.

Although we attempted to isolate the mRGC function using the silent-substitution

technique, the cone signals contaminated the pupillary response to test stimuli with the onset of the square-wave envelope due to the high sensitivity component at the abrupt change of the stimulus. On the other hand, since sensitivity of cones is much lower for the test stimuli with onset of sinusoidal envelope than that of mRGCs, the pupillary response to the mRGC stimulus was determined by mRGCs, while the response to the luminance stimuli was determined by the cone-mediated signals.

Figure 7

Figure 8

DISCUSSION

The delayed pupillary response to mRGC stimuli

The delayed pupillary response was found when responses to the mRGC stimuli with onset of sinusoidal envelope were compared to the luminance stimuli, suggesting the contribution of the mRGCs. In a study using transgenic animals, Lucas et al. measured pupil light reflex in mice lacking rods and cones (i.e., mRGCs only) and compared the results with those in wild-type mice (Lucas et al, 2001). The mice lacking cones and

rods had a latency of ~730 ms whereas the wild type mice had a latency of ~450 ms. The difference in latency was approximately ~280 ms. Our results showed that a difference in time when initiating constriction between the mRGC and the light flux condition was 189 ms and the difference in time to the peak was 131 ms. In humans, the pupillary responses to luminance and chromatic stimuli were different, suggesting a contribution of post-receptoral mechanisms such as |L+M| luminance and |L-M| cone-opponent mechanisms to the pupillary pathway (e.g., Barbur et al, 1998; Tsujimura et al, 2001). The difference in latency obtained in our experiments could reflect a difference between signals from post-receptoral mechanisms and mRGCs as opposed to signals from cones and mRGCs in humans. Although the contribution of signals in luminance and chromatic pathways which physiologically corresponds to Magno- and Parvo-cellular pathways is well known in visual psychophysics it is not yet clear how these conventional retinal ganglion cells contribute to the pupillary pathway (e.g., Guler et al, 2008). One of the reasons could be due to a large contribution of mRGCs to the pupillary pathway and importantly most of previous researches were done without consideration of mRGCs. Although the neural mechanisms of these conventional retinal ganglion cells and mRGCs associated with pupillary response are interesting the difference in latency obtained under the isolation of post-receptoral mechanisms and

mRGCs, therefore, should be a matter for future research. Although the latencies obtained in our experiments were slightly shorter than those in the mice study, they are generally consistent. The results of the present study showed that we successfully demonstrated the pupillary response to mRGCs under conditions where mRGCs are isolated in humans.

The post-stimulus pupillary constriction

Gamlin et al. measured the pupillary response to a test stimulus with duration of 10 seconds and found that the pupil had a sustained constriction in darkness after the offset of the test stimulus (Gamlin et al, 2007). They showed that the action spectrum of this post-stimulus pupil constriction was well fit by the melanopsin nomogram with a peak wavelength of 483 nm, indicating that this post-stimulus pupil constriction is mediated by melanopsin-associated signals. In our experiment, the pupil response to the mRGC stimulus with onset of sinusoidal envelope, however, cannot provide a unified and coherent evidence for a sustained pupil constriction after the offset of test stimulus. Gamlin et al. presented a bright test stimulus in darkness and measured pupil response. The test stimulus induced a very large pupil response of about 1.5 mm. On the other hand, we presented a test stimulus modulated on a bright background with low contrast

in the silent-substitution paradigm. The color and luminance for the mRGC stimulus were the same as those for the background, which were the so-called metamers that have the same tristimulus values but different spectral radiant power distributions. Although no truly satisfactory explanation how mRGCs produce post-stimulus pupil constriction has been found, it seems that such a mechanism could require a large change in stimulus, and hence our test stimulus might not induce post-stimulus pupil constriction.

Interaction of mRGC and cone-mediated signals

In our experiment, the L-cone and M-cone contrasts were the same between the luminance and the light flux stimuli whereas the mRGC and S-cone contrasts were different. The L-cone, M-cone, S-cone and mRGC contrasts were 0.14, 0.09, 0.06, and 0.04 for the light flux stimuli and 0.14, 0.09, 0.00, and 0.00 for the luminance stimuli. Since the S cones have a weak contribution to the pupillary pathway (e.g., Verdon and Howarth, 1988), the difference in pupillary response between the luminance and the light flux stimuli, therefore, could be used to estimate the contribution of mRGCs to the pupillary responses.

There was no significant difference in amplitude between the luminance and light flux

stimuli for the onset of sinusoidal stimuli. This result suggests a small contribution of mRGCs or a negative functional interaction between mRGCs and cones to the pupillary responses. The amplitude of the responses to the mRGC stimulus for the onset of sinusoidal envelope was relatively large and similar to those for the luminance and the light flux stimuli with a mRGC contrast of 0.08. This paradox could simply be explained by the fact that there is a latency difference in pupillary response between mRGC and cone-mediated signals. We have shown that there was a significant difference in latency between mRGC and the luminance and the light flux stimuli. It is evident that the latency difference needs to be considered when investigating an interaction of mRGC signals and cone-mediate signals.

FIGURE CAPTIONS

Figure 1

Experimental setup. A personal computer controlled the stimulation system, which consisted of two integrating spheres; one for test stimulus presentation and the other for background presentation. The test field was an annular ring and the background field was a circular field. The test stimulus was superposed on the background using a beam splitter. Luminance output of each LED was controlled by pulse width modulation (PWM) units by adjusting the duty cycle of the pulse train at 1 kHz. The PWM units were controlled by an embedded computer.

Figure 2

The temporal waveforms (upper panel) and the spectra (lower panel) for sinusoidal and square-wave stimuli.

Figure 3

The pupil response to the onset of sinusoidal stimuli for two observers. The solid curve represents response to the mRGC stimulus, the dotted curve represents responses to the luminance stimulus, and the broken curve represents responses to the light flux stimulus. The temporal envelope of the test stimuli is shown by the grey area on the time-scale axis.

Figures 4 and 5

The pupil response to the onset of sinusoidal stimuli for two observers. Figure 4 shows onset latencies and Fig. 5 shows enlarged ones. The amplitude of the pupillary response to mRGC, luminance, and light flux stimuli were normalized with respect to average amplitude and the trace overlaid such that the difference in latency could be detected. All other details are the same as those in Fig. 3

Figure 6

The pupil response to the onset of square-wave stimuli for two observers. The solid curve represents response to the mRGC stimulus, the dotted curve represents responses to the luminance stimulus, and the broken curve represents responses to the light flux stimulus. All other details are the same as those in Fig. 3.

Figures 7 and 8

The pupil response to the onset of square-wave stimuli for two observers. The amplitude of the pupillary response to mRGC, luminance, and the light flux stimuli were normalized with respect to the average amplitude and the trace overlaid such that the difference in latency could be detected. All other details are the same as those in Fig. 6.

Table 1

The summary of latencies and amplitudes of the pupil response for all observers. The

upper panel represents values for sinusoidal stimuli and the lower panel represents values for square-wave stimuli.

REFERENCES

Aguilar, M. and Stiles, W. S. (1954) Saturation of the rod mechanism of the retina at high levels of stimulation. *Journal. of. Modern. Optics. Taylor. &. Francis.*, **1**, 59-65.

Alpern, M. and Ohba, N. (1972) The effect of bleaching and backgrounds on pupil size. *Vision. Res.*, **12**, 943-951.

Barbur, J. L., Wolf, J. and Lennie, P. (1998) Visual processing levels revealed by response latencies to changes in different visual attributes. *Proc. Biol. Sci.*, **265**, 2321-2325.

Berson, D. M., Dunn, F. A. and Takao, M. (2002) Phototransduction by retinal ganglion cells that set the circadian clock. *Science.*, **295**, 1070-1073.

Brainard, G. C., Hanifin, J. P., Greeson, J. M., Byrne, B., Glickman, G., Gerner, E. and Rollag, M. D. (2001) Action spectrum for melatonin regulation in humans: evidence for a novel circadian photoreceptor. *J. Neurosci.*, **21**, 6405-6412.

Cao, D., Pokorny, J., Smith, V. C. and Zele, A. J. (2008) Rod contributions to color perception: linear with rod contrast. *Vision. Res.*, **48**, 2586-2592.

Dacey, D. M., Liao, H. W., Peterson, B. B., Robinson, F. R., Smith, V. C., Pokorny, J., Yau, K. W. and Gamlin, P. D. (2005) Melanopsin-expressing ganglion cells in primate retina signal colour and irradiance and project to the LGN. *Nature.*, **433**, 749-754.

Dartnall, H. J. (1953) The interpretation of spectral sensitivity curves. *Br. Med. Bull.*, **9**, 24-30.

De Lange, H. (1954) Relationship between critical flicker-frequency and a set of low-frequency characteristics of the eye. *J. Opt. Soc. Am.*, **44**, 380-388.

Do, M. T., Kang, S. H., Xue, T., Zhong, H., Liao, H. W., Bergles, D. E. and Yau, K. W. (2009) Photon capture and signalling by melanopsin retinal ganglion cells. *Nature.*, **457**, 281-287.

Freedman, M. S., Lucas, R. J., Soni, B., von Schantz, M., Munoz, M., David-Gray, Z. and Foster, R. (1999) Regulation of mammalian circadian behavior by non-rod, non-cone, ocular photoreceptors. *Science.*, **284**, 502-504.

Fuortes, M. G., Gunkel, R. D. and Rushton, W. A. (1961) Increment thresholds in a subject deficient in cone vision. *J. Physiol.*, **156**, 179-192.

Gamlin, P. D., McDougal, D. H., Pokorny, J., Smith, V. C., Yau, K. W. and Dacey, D. M. (2007) Human and macaque pupil responses driven by melanopsin-containing retinal ganglion cells. *Vision. Res.*, **47**, 946-954.

Guler, A. D., Ecker, J. L., Lall, G. S., Haq, S., Altimus, C. M., Liao, H. W., Barnard, A.

R., Cahill, H., Badea, T. C., Zhao, H., Hankins, M. W., Berson, D. M., Lucas, R. J., Yau, K. W. and Hattar, S. (2008) Melanopsin cells are the principal conduits for rod-cone input to non-image-forming vision. *Nature.*, **453**, 102-105.

Hansen, R. M. and Fulton, A. B. (1986) Pupillary changes during dark adaptation in human infants. *Invest. Ophthalmol. Vis. Sci.*, **27**, 1726-1729.

Hattar, S., Liao, H. W., Takao, M., Berson, D. M. and Yau, K. W. (2002) Melanopsin-containing retinal ganglion cells: architecture, projections, and intrinsic photosensitivity. *Science.*, **295**, 1065-1070.

Hattar, S., Lucas, R. J., Mrosovsky, N., Thompson, S., Douglas, R. H., Hankins, M. W., Lem, J., Biel, M., Hofmann, F., Foster, R. G. and Yau, K. W. (2003) Melanopsin and rod-cone photoreceptive systems account for all major accessory visual functions in mice. *Nature.*, **424**, 76-81.

Kardon, R., Anderson, S. C., Damarjian, T. G., Grace, E. M., Stone, E. and Kawasaki, A. (2009) Chromatic pupil responses: preferential activation of the melanopsin-mediated versus outer photoreceptor-mediated pupil light reflex. *Ophthalmology.*, **116**, 1564-1573.

Kardon, R., Anderson, S. C., Damarjian, T. G., Grace, E. M., Stone, E. and Kawasaki, A. (2010) Chromatic Pupillometry in Patients with Retinitis Pigmentosa. *Ophthalmology. 2010. Sep.*, , 22.

Lall, G. S., Revell, V. L., Momiji, H., Al Enezi, J., Altimus, C. M., Guler, A. D., Aguilar, C., Cameron, M. A., Allender, S., Hankins, M. W. and Lucas, R. J. (2010) Distinct contributions of rod, cone, and melanopsin photoreceptors to encoding irradiance. *Neuron.*, **66**, 417-428.

Lamb, T. D. (1995) Photoreceptor spectral sensitivities: common shape in the long-wavelength region. *Vision. Res.*, **35**, 3083-3091.

Lee, B. B., Smith, V. C., Pokorny, J. and Kremers, J. (1997) Rod inputs to macaque ganglion cells. *Vision. Res.*, **37**, 2813-2828.

Lucas, R. J., Freedman, M. S., Munoz, M., Garcia-Fernandez, J. M. and Foster, R. G. (1999) Regulation of the mammalian pineal by non-rod, non-cone, ocular photoreceptors. *Science.*, **284**, 505-507.

Lucas, R. J., Douglas, R. H. and Foster, R. G. (2001) Characterization of an ocular photopigment capable of driving pupillary constriction in mice. *Nat. Neurosci.*, **4**, 621-626.

Lucas, R. J., Hattar, S., Takao, M., Berson, D. M., Foster, R. G. and Yau, K. W. (2003) Diminished pupillary light reflex at high irradiances in melanopsin-knockout mice. *Science.*, **299**, 245-247.

McDougal, D. H. and Gamlin, P. D. (2010) The influence of intrinsically-photosensitive retinal ganglion cells on the spectral sensitivity and response dynamics of the human pupillary light reflex. *Vision. Res.*, **50**, 72-87.

Mrosovsky, N. and Hattar, S. (2003) Impaired Masking Responses to Light in Melanopsin-Knockout Mice. *Chronobiology. International.*, **20**, 989-999.

Panda, S., Sato, T. K., Castrucci, A. M., Rollag, M. D., DeGrip, W. J., Hogenesch, J. B., Provencio, I. and Kay, S. A. (2002) Melanopsin (Opn4) requirement for normal light-induced circadian phase shifting. *Science.*, **298**, 2213-2216.

Panda, S., Provencio, I., Tu, D. C., Pires, S. S., Rollag, M. D., Castrucci, A. M., Pletcher, M. T., Sato, T. K., Wiltshire, T., Andahazy, M., Kay, S. A., Van Gelder, R. N. and Hogenesch, J. B. (2003) Melanopsin is required for non-image-forming photic responses in blind mice. *Science.*, **301**, 525-527.

Pokorny, J., Smithson, H. and Quinlan, J. (2004) Photostimulator allowing independent control of rods and the three cone types. *Vis. Neurosci.*, **21**, 263-267.

Provencio, I., Jiang, G., De Grip, W. J., Hayes, W. P. and Rollag, M. D. (1998) Melanopsin: An opsin in melanophores, brain, and eye. *Proc. Natl. Acad. Sci. U. S. A.*, **95**, 340-345.

Provencio, I., Rodriguez, I. R., Jiang, G., Hayes, W. P., Moreira, E. F. and Rollag, M. D. (2000) A novel human opsin in the inner retina. *J. Neurosci.*, **20**, 600-605.

Provencio, I., Rollag, M. D. and Castrucci, A. M. (2002) Photoreceptive net in the mammalian retina. This mesh of cells may explain how some blind mice can still tell day from night. *Nature.*, **415**, 493.

Ruby, N. F., Brennan, T. J., Xie, X., Cao, V., Franken, P., Heller, H. C. and O'Hara, B. F. (2002) Role of melanopsin in circadian responses to light. *Science.*, **298**, 2211-2213.

Shapiro, A. G., Pokorny, J. and Smith, V. C. (1996) Cone-rod receptor spaces with illustrations that use CRT phosphor and light-emitting-diode spectra. *J. Opt. Soc. Am. A. Opt. Image. Sci. Vis.*, **13**, 2319-2328.

Smith, V. C. and Pokorny, J. (1996) The design and use of a cone chromaticity space: A tutorial. *Color. Research. &. Application.*, **21**, 375-383.

Stockman, A., Sharpe, L. T. and Fach, C. (1999) The spectral sensitivity of the human short-wavelength sensitive cones derived from thresholds and color matches. *Vision. Res.*, **39**, 2901-2927.

Stockman, A. and Sharpe, L. T. (2000) The spectral sensitivities of the middle- and long-wavelength-sensitive cones derived from measurements in observers of known genotype. *Vision. Res.*, **40**, 1711-1737.

Thapan, K., Arendt, J. and Skene, D. J. (2001) An action spectrum for melatonin suppression: evidence for a novel non-rod, non-cone photoreceptor system in humans. *J. Physiol.*, **535**, 261-267.

Tsujimura, S., Wolffsohn, J. S. and Gilmartin, B. (2001) A linear chromatic mechanism drives the pupillary response. *Proc. Biol. Sci.*, **268**, 2203-2209.

Tsujimura, S., Wolffsohn, J. S. and Gilmartin, B. (2003) Pupil responses associated with coloured afterimages are mediated by the magno-cellular pathway. *Vision. Res.*, **43**, 1423-1432.

Tsujimura, S., Shioiri, S. and Nuruki, A. (2007) Two distinct cone-opponent processes in the L+ M luminance pathway. *Vision. Research.*, **47**, 1839-1854.

Tsujimura, S., Ukai, K., Ohama, D., Nuruki, A. and Yunokuchi, K. (2010) Contribution of human melanopsin retinal ganglion cells to steady-state pupil responses. *Proc. Biol. Sci.*, **277**, 2485-2492.

Verdon, W. and Howarth, P. A. (1988) The pupil's response to short wavelength cone stimulation. *Vision. Res.*, **28**, 1119-1128.

Vienot, F., Bailacq, S. and Rohellec, J. L. (2010) The effect of controlled photopigment excitations on pupil aperture. *Ophthalmic. Physiol. Opt.*, **30**, 484-491.

Watanabe, T., Mori, N. and Nakamura, F. (1992) A new superbright LED stimulator: photodiode-feedback design for linearizing and stabilizing emitted light. *Vision. Res.*, **32**, 953-961.

Wyszecki, G. and Stiles, W. S. (1982) Color science: concepts and methods, quantitative data and formulae *New. York.*, , J. Wiley.

Young, R. S. and Kimura, E. (2008) Pupillary correlates of light-evoked melanopsin activity in humans. *Vision. Res.*, **48**, 862-871.

Zaidi, F. H., Hull, J. T., Peirson, S. N., Wulff, K., Aeschbach, D., Gooley, J. J., Brainard, G. C., Gregory-Evans, K., Rizzo, J.F. 3rd, Czeisler, C. A., Foster, R. G., Moseley, M. J. and Lockley, S. W. (2007) Short-wavelength light sensitivity of circadian, pupillary, and visual awareness in humans lacking an outer retina. *Curr. Biol.*, **17**, 2122-2128.

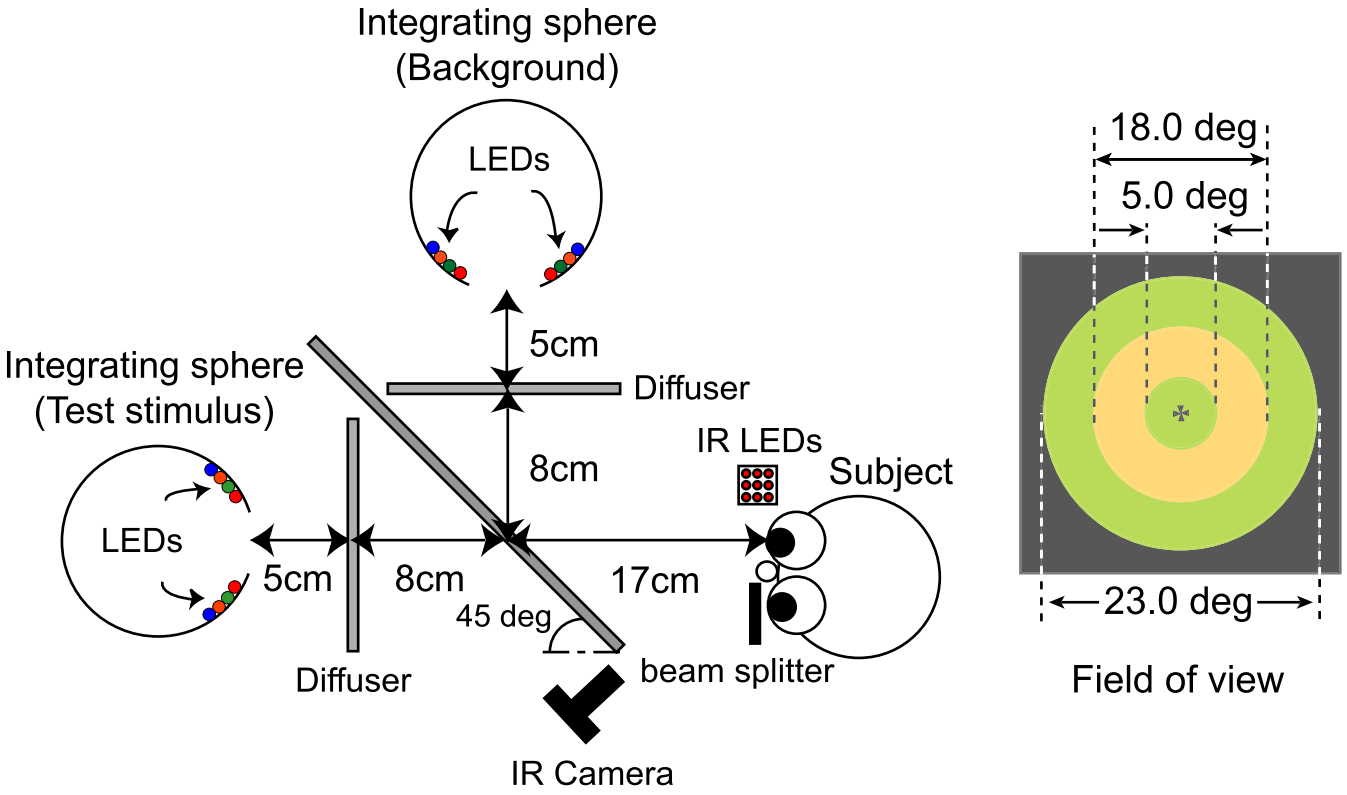
Integrating sphere
(Background)
LEDs
5cm
Diffuser
Integrating sphere
(Test stimulus)
8cm
IR LEDs
Subject
LEDs
5cm
8cm
17cm
45 deg
Diffuser
beam splitter
IR Camera
18.0 deg
5.0 deg
23.0 deg
Field of view

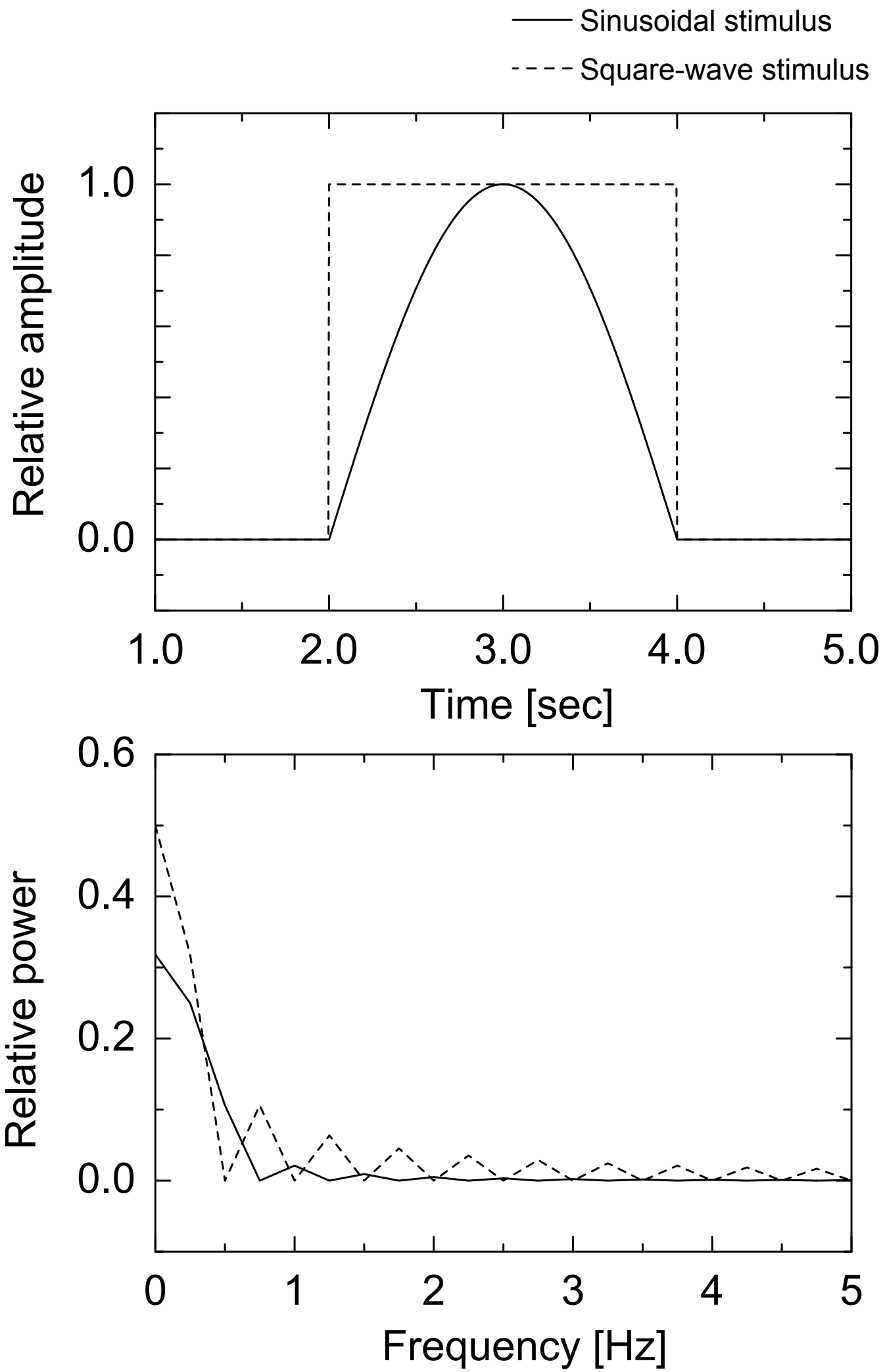
Sinusoidal stimulus
Square-wave stimulus
Relative amplitude
1.0
0.0
1.0
2.0
3.0
4.0
5.0
Time [sec]
Relative power
0.6
0.4
0.2
0.0
0
1
2
3
4
5
Frequency [Hz]

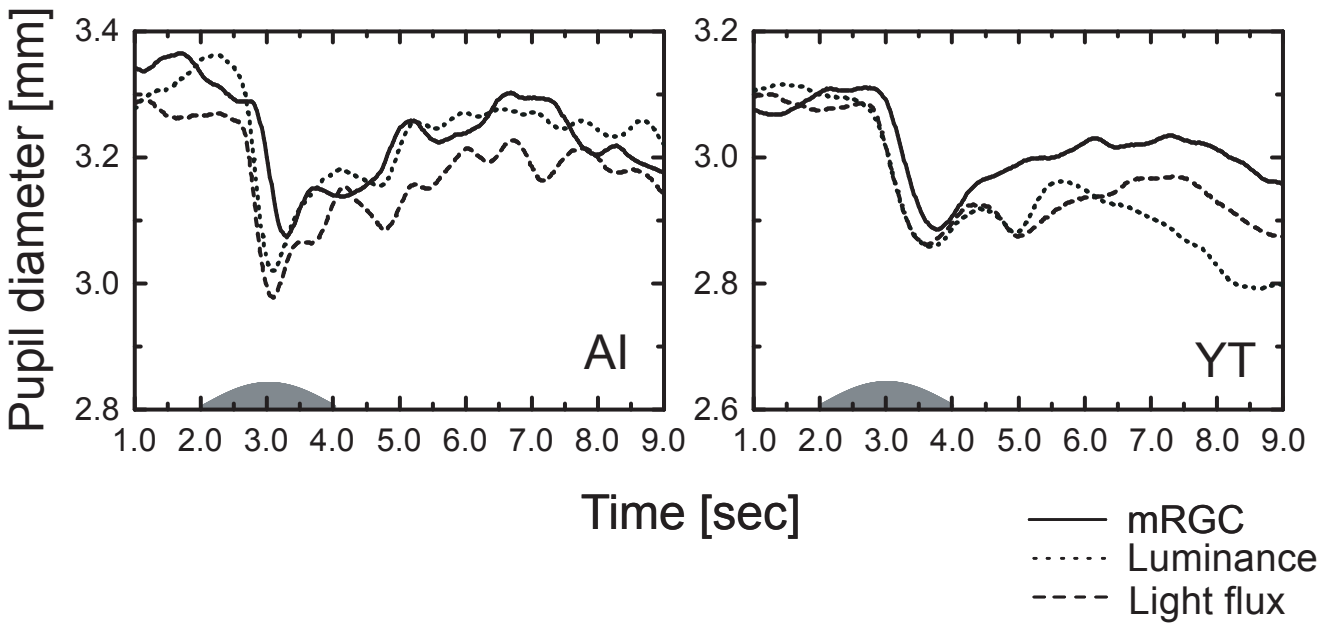
Pupil diameter [mm]
3.4
3.2
3.0
2.8
AI
1.0 2.0 3.0 4.0 5.0 6.0 7.0 8.0 9.0
3.2
3.0
2.8
2.6
YT
1.0 2.0 3.0 4.0 5.0 6.0 7.0 8.0 9.0
Time [sec]
mRGC
Luminance
Light flux

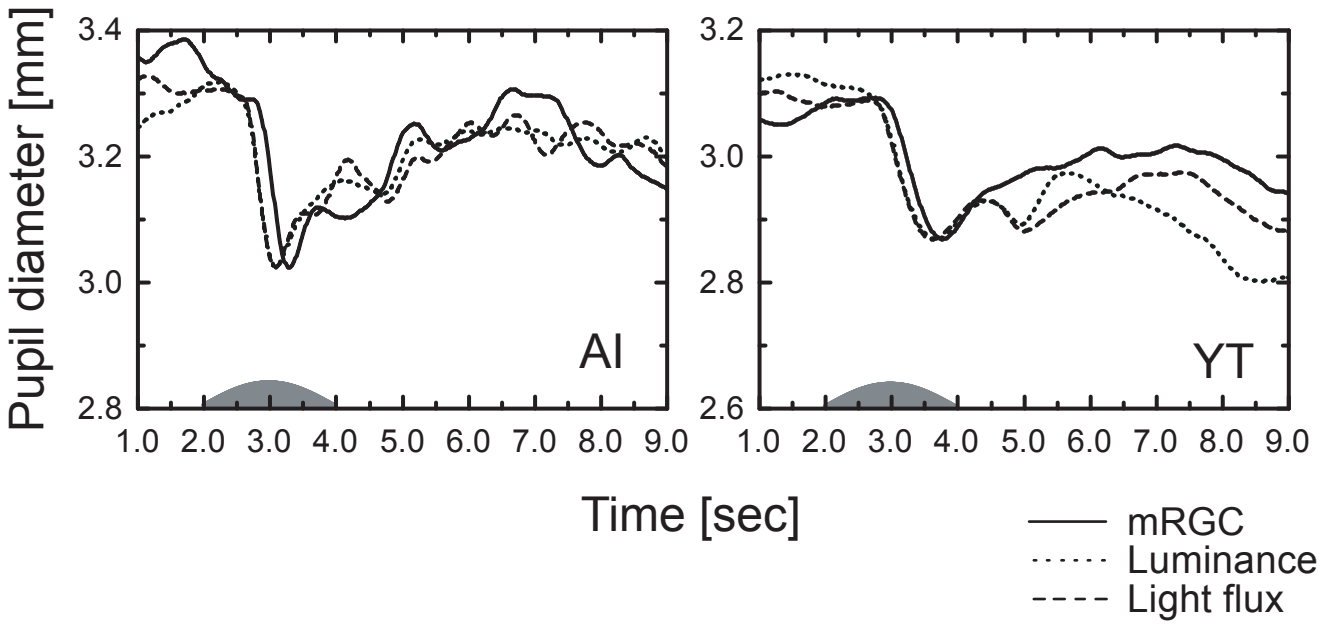
Pupil diameter [mm]
3.4
3.2
3.0
2.8
AI
1.0 2.0 3.0 4.0 5.0 6.0 7.0 8.0 9.0
3.2
3.0
2.8
2.6
YT
1.0 2.0 3.0 4.0 5.0 6.0 7.0 8.0 9.0
Time [sec]
mRGC
Luminance
Light flux

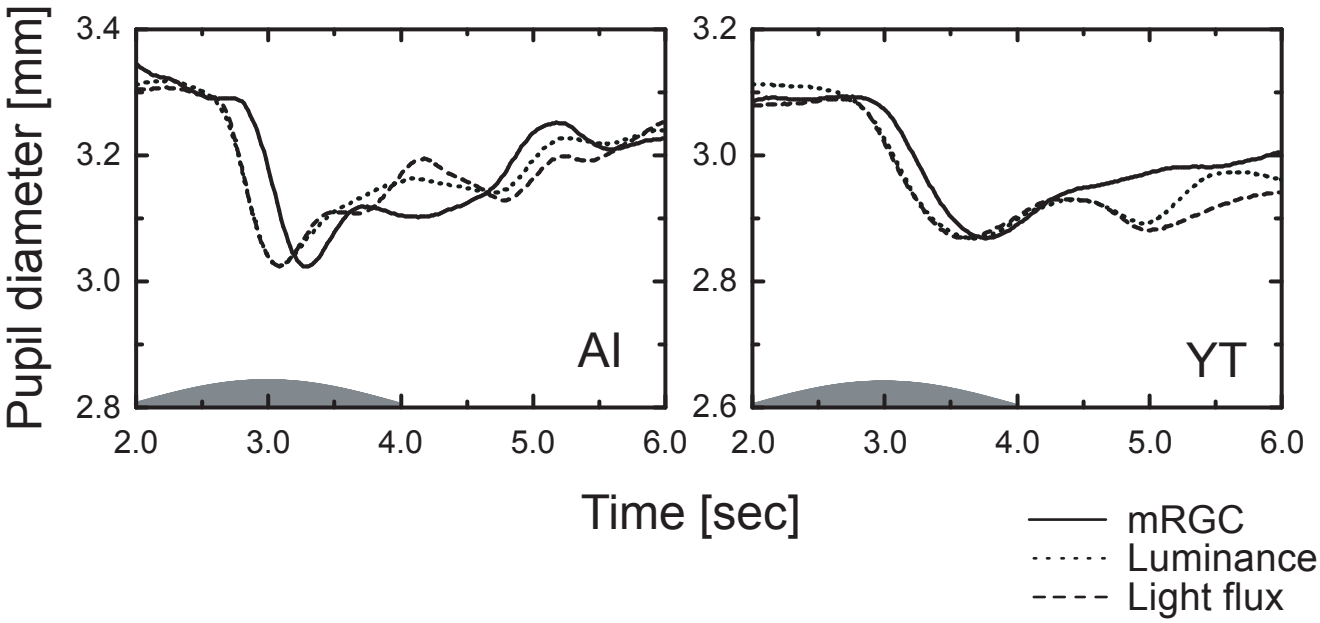
Pupil diameter [mm]
3.4
3.2
3.0
2.8
AI
2.0
3.0
4.0
5.0
6.0
3.2
3.0
2.8
2.6
YT
2.0
3.0
4.0
5.0
6.0
Time [sec]
mRGC
Luminance
Light flux

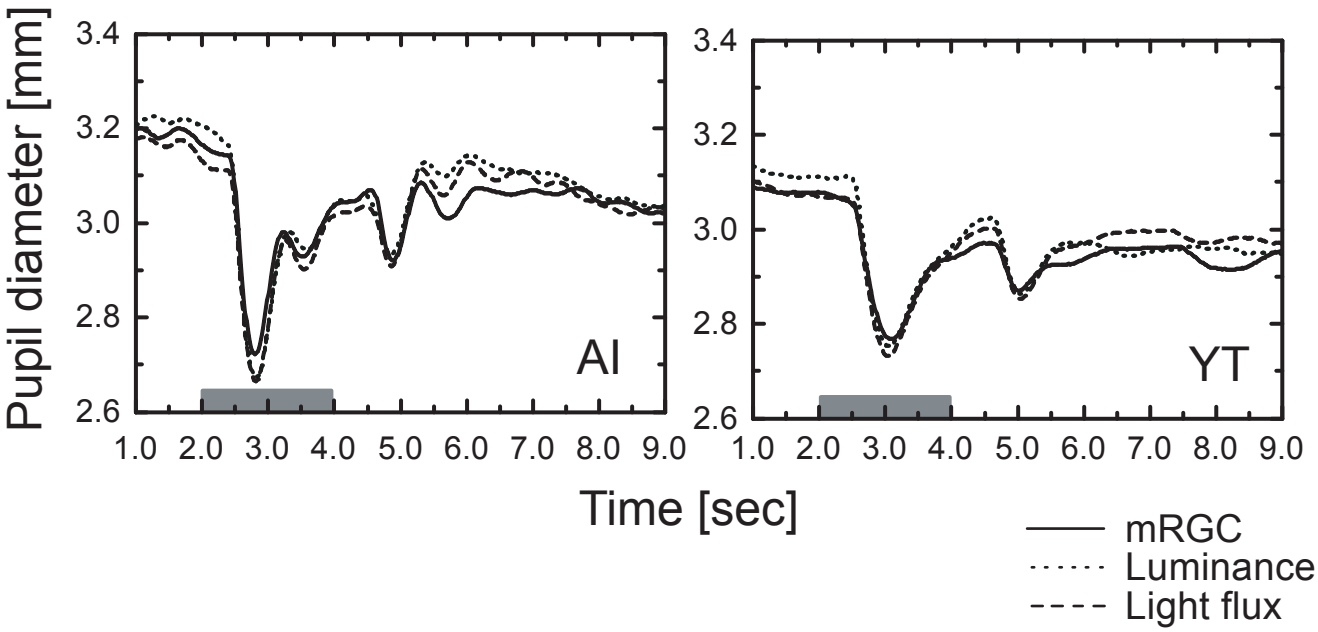
Pupil diameter [mm]
3.4
3.2
3.0
2.8
2.6
1.0 2.0 3.0 4.0 5.0 6.0 7.0 8.0 9.0
AI
YT
Time [sec]
mRGC
Luminance
Light flux

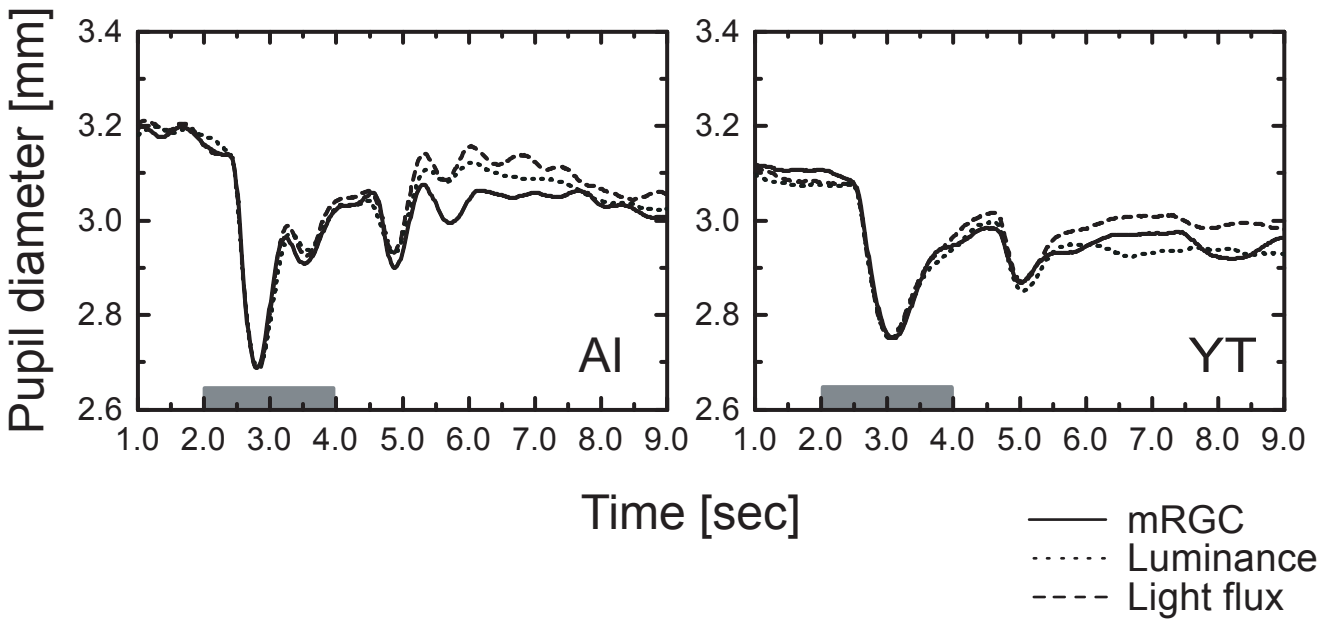
Pupil diameter [mm]
3.4
3.2
3.0
2.8
2.6
1.0 2.0 3.0 4.0 5.0 6.0 7.0 8.0 9.0
AI
YT
Time [sec]
mRGC
Luminance
Light flux

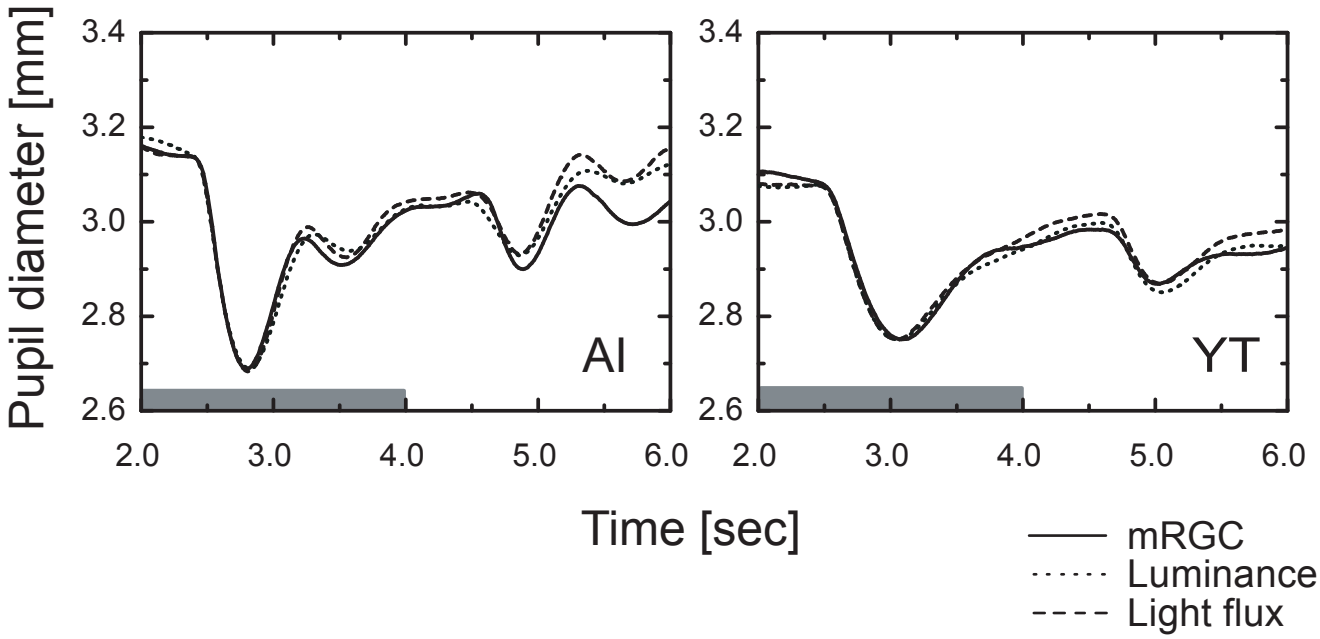
Pupil diameter [mm]
3.4
3.2
3.0
2.8
2.6
2.0
3.0
4.0
5.0
6.0
AI
YT
Time [sec]
mRGC
Luminance
Light flux